JOURNAL OF AGRICULTURAL AND FOOD CHEMISTRY

Kinetic Study of the Oxidation of Quercetin by Mushroom Tyrosinase

LORENA G. FENOLL,[†] PEDRO A. GARCÍA-RUIZ,[‡] RAMÓN VARÓN,[§] AND FRANCISCO GARCÍA-CÁNOVAS*,[†]

GENZ, Grupo de Investigación Enzimología, and Departamento de Bioquímica y Biología Molecular-A, Facultad de Biología, Universidad de Murcia, A. Correos 4021, E-30080 Murcia, Spain, Departamento de Química Orgánica, Facultad de Química, Universidad de Murcia, Murcia, Spain, and Departamento de Química Física, Escuela Técnica Superior de Albacete, Universidad de Castilla-La Mancha, Albacete, Spain

The kinetic behavior of mushroom tyrosinase in the presence of the flavonol quercetin was studied. This flavonol was oxidized by mushroom tyrosinase and the reaction was followed by recording spectral changes over time. The spectra obtained during the reaction showed two isosbectic points, indicating a stable *o*-quinone. When quercetin was oxidized by tyrosinase in the presence of cysteine and 3-methyl-2-benzothiazolone hydrazone (Besthorn's hydrazone, MBTH) isosbestic points were also observed indicating a definite stoichiometry. From the data analysis of the initial rate in the presence of MBTH, the kinetic parameters: $V_{max}^{app} = (16.2 \pm 0.6)\ \mu$M/min, $K_m^{app} = (0.12 \pm 0.01)$ mM, $(V_{max}^{app}/K_m^{app}) = (V_{max}/K_{S'}) = (13.5 \pm 1.4) \times 10^{-2}$ min^{-1}, $k_{cat}^{app} = (6.2 \pm 0.6)$ s^{-1} were determined. We propose that quercetin acts simultaneously as a substrate and a rapid reversible inhibitor of mushroom tyrosinase, depending on how it binds to the copper atom of the enzyme active site. Thus, if the binding occurs through the hydroxylic groups at the C3′ and C4′ positions, quercetin acts as a substrate, while if it occurs through the hydroxylic group at the C3 position of the pyrone ring, quercetin acts as an inhibitor.

KEYWORDS: Tyrosinase; flavonol; polyphenol oxidase; quercetin; spectrophotometry

INTRODUCTION

Tyrosinase or polyphenoloxidase (EC 1.14.18.1) is a copper enzyme widely distributed throughout the phylogenetic scale (*1*−*5*). It catalyses the hydroxylation of monophenols to *o*-diphenols and their subsequent oxidation to *o*-quinones, in both cases by molecular oxygen. The enzyme is responsible for skin, eye, inner ear, and hair melanization (*6*, *7*) and enzymatic browning in fruits and vegetables (*8*−*10*). Tyrosinase also has industrial applications in the preparation of biosensors for oxygen and phenols, in the stereospecific synthesis of phenols and polymers, and in the bioremediation of wastes contaminated by phenols (*2*, *11*).

Tyrosinase exhibits wide substrate specificity, and recently attention has focused on polyphenols with complex structures, such as flavonoids. These natural polyphenols are widely distributed in fruit and vegetables (*12*) and have multiple chemical and biological functions, acting as antioxidants (*13*), chelating agents (*14*), anticarcinogenics and bacteriostatics (*15*). Recent investigations point to the tyrosinase inhibitory activity of flavonols, such as quercetin, kaempferol, and morin (*16*, *17*). In these flavonoids, with a free 3-hydroxyl group, a chelation mechanism acting on the copper atoms of the active site of the enzyme has been proposed (*16*, *17*). Moreover, it has been proposed that quercetin acts as a single-step time-dependent inhibitor of mushroom tyrosinase (*17*).

For some time, the time-dependent inhibition of tyrosinase from several sources by the inhibitors, *m*-coumaric acid (*18*), L-mimosine (*19*), kojic acid (*20*), and tropolone, (*21*) has been studied. The common characteristic of these inhibitors, are hydroxyl groups that cannot be oxidized by the enzyme. An inhibition mechanism based on binding to the copper atoms of the enzyme has been proposed. Such an inhibition mechanism has been assumed to act in two steps: a fast enzyme binding step followed by a slow first-order transition (*18*−*21*).

To confirm whether quercetin acts via a one-step time-dependent inhibition mechanism, as has been proposed (*17*), or a two-step mechanism as described in (*18*−*21*), we have carried out a kinetic study of the oxidation of L-dopa by mushroom tyrosinase in the presence and absence of quercetin. In addition, we have studied the possible oxidation of quercetin by mushroom tyrosinase, and the results showed that quercetin is a tyrosinase substrate. Because quercetin has a free hydroxyl group at the 3-position, this compound can also act as an inhibitor. Thus, this molecule is simultaneously a substrate and an inhibitor, depending on the way in which it binds to the copper atoms of the active site.

* To whom correspondence should be addressed. Tel.: +34968364782. Fax: +34968363963. E-mail:canovasf@um.es.
[†] GENZ.
[‡] Universidad de Murcia.
[§] Universidad de Castilla-La Mancha.

10.1021/jf034656y CCC: $25.00
Published on Web 11/18/2003

MATERIALS AND METHODS

Reagents. Quercetin was purchased from Aldrich (Madrid, Spain), and dimethyl sulfoxide (DMSO) and L-dopa from Sigma (Madrid, Spain). A stock solution of quercetin was prepared in DMSO and a stock solution of the L-dopa was prepared in 0.15 mM phosphoric acid to prevent autoxidation. Milli-Q system (Millipore Corp., Spain) ultrapure water was used throughout this research. These solutions were further purified by Chelex-100 chromatography (100−200 mesh, Na^+ form, BioRad) to remove traces of metal ions.

Enzyme. Mushroom tyrosinase (5350 U/mg) was purchased from Sigma (Madrid, Spain) and purified by Duckworth and Coleman's procedure with some modifications (*22*, *23*). The enzyme concentration was calculated assuming $M_r = 120\,000$ Da. Protein content was determined by Bradford's method (*24*) using bovine serum albumin as standard.

Oxymetric Assays. The O_2 concentration was determined by using a Clark electrode with a Hansatech (Kings Lynn, UK) oxymeter, interfaced to a PC-compatible computer running Quiceltron software. The electrode was previously calibrated using the tyrosinase-catalyzed O_2-dependent oxidation of *tert*-butylcatechol (TBC) (*25*).

Spectrophotometric Assays. Kinetic assays were carried out by measuring the appearance of the product in the reaction medium in a Perkin-Elmer Lambda-2 UV−vis spectrophotometer controlled using Perkin-Elmer UV−Winlab software. The temperature was controlled at 25 °C ± 0.1 °C using a Haake D1G circulating water-bath checked using a Cole-Parmer digital thermometer. Reference cuvettes contained all the components except the substrate, with a final volume of 1 mL. Substrate concentration, buffer and other assay conditions are indicated in the legend to each figure. All the assays were carried out under conditions of tyrosinase saturation by molecular oxygen, (0.26 mM in the assay medium) (*26*). The quercetin oxidation reaction was followed at 510 nm by measuring the MBTH−quercetin adduct. In the case of L-dopa oxidation, the wavelength used was 475 nm, and when the reaction was carried out in the presence of quercetin, the wavelength used was 515 nm to avoid interference due to quercetin absorbance, in the presence of MBTH, the reaction was registered at 484 nm.

Determination of the Molar Absorptivity Coefficient of the MBTH−Quercetin Adduct. To obtain quantitative initial rate data, it was necessary to determine the molar absorptivity coefficient at 510 nm ($\epsilon_{510\ nm}$) of the MBTH−quercetin adduct. The method that we propose consists of the measuring adduct absorbance, which is formed stoichiometrically, accompanied by O_2 consumption (which is limiting), during the reaction of tyrosinase with quercetin. This method was previously used by us to calculate the molar absorptivities of the thiol-diphenol adducts (*27*). The assay conditions are [quercetin] ≫ $[O_2]_0$, [MBTH] ≫ $[O_2]_0$, and the reaction stoichiometry is

$$1\ O_2 + 2\ \text{quercetin} + 2\ \text{MBTH} \rightarrow 2\ \text{MBTH−quercetin} + 2\ H_2O$$

The standard mixture contained quercetin and MBTH in 50 mM sodium phosphate buffer, pH 7.0, through which nitrogen gas was bubbled prior to use. The reaction was started by injection of an enzyme sample containing a known concentration of oxygen. The cuvette was then rapidly closed with a Teflon stopper. The increase in absorbance was determined spectrophotometrically. The representation of the absorbance increase vs the O_2 concentration added in the assays, permitted the determination of the molar absorptivity coefficient, as described below. The value obtained was $e_{510} = 1509\ M^{-1}cm^{-1}$.

Kinetic Data Analysis. Experimental data points are the mean values of triplicate assays. The error bars corresponding to the standard deviation interval are the same size as the diameter of the symbols used in the plots (*28*).

NMR Assays. The ^{13}C NMR spectrum of quercetin was obtained in a Varian Unity 300 MHz spectrometer, using deuterated DMSO as solvent. δ values were measured relative to those for tetramethylsilane ($\delta = 0$). The maximum line width accepted in the NMR spectra was 0.06 Hz. Therefore, the maximum accepted error for each peak was ± 0.03 ppm.

Scheme 1. Chemical Structures of Quercetin, Tropolone, L-Mimosine and Kojic Acid

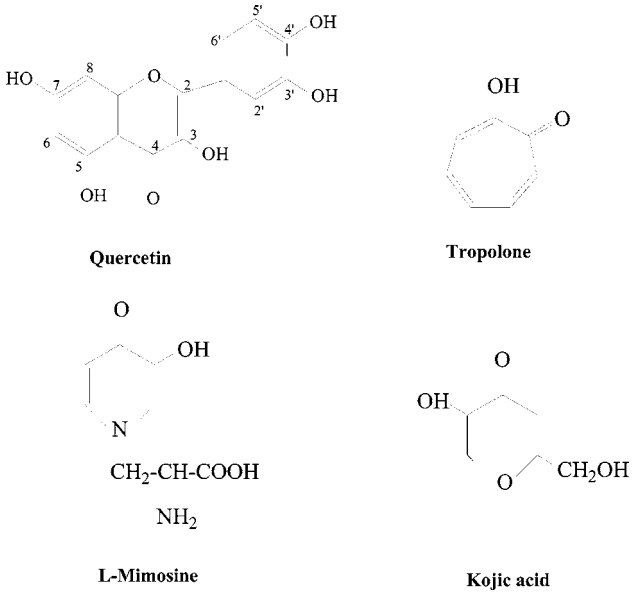

RESULTS AND DISCUSSION

Chemical Structure of Quercetin. When the chemical structure of the flavonol quercetin depicted in **Scheme 1** is taken into account, the presence of *ortho*-hydroxyl groups suggests that this compound may act as a substrate of mushroom tyrosinase. **Figure 1** shows the spectrum of quercetin with a maximum at 375 nm. The presence of the heterocycle with a carbonyl group and an *ortho*-hydroxylic group recalls the structures of L-mimosine, kojic acid, and tropolone (**Scheme 1**), all of which have been characterizated as time-dependent inhibitors of tyrosinase from several sources, acting in two steps (*18*−*21*). However, *m*-coumaric acid (*18*) and kojic acid (*20*) only act as time-dependent inhibitors on frog epidermis tyrosinase and not on mushroom tyrosinase.

Oxidation of L-dopa by mushroom tyrosinase in the absence and presence of quercetin

Figure 2 shows the spectrophotometric recordings of L-dopa oxidation by mushroom tyrosinase in the absence (**a**) and presence (**b**) of quercetin, and the same experiments with the

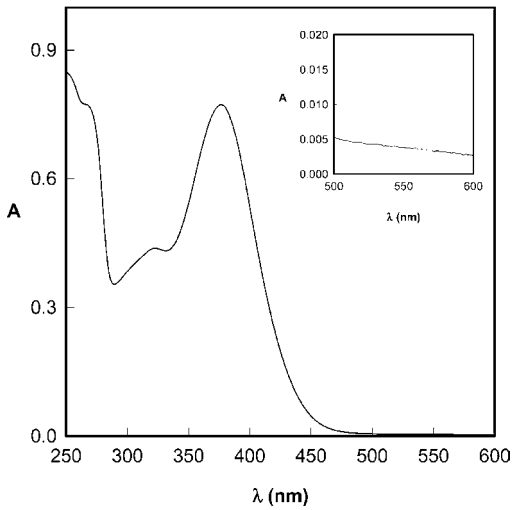

Figure 1. Spectrum of quercetin. The assay medium (1 mL) contained 45 μM quercetin and 50 mM sodium phosphate buffer, pH 7.0, at 25 °C. Inset: Wavelength amplification between 500 and 600 nm.

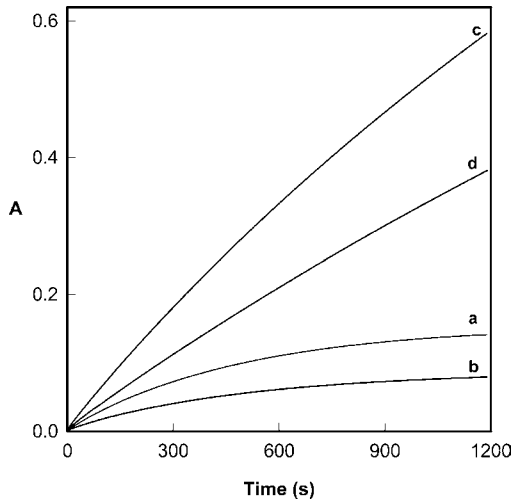

Figure 2. Spectrophotometric recordings of tyrosinase action on (a) L-dopa, (b) L-dopa in the presence of quercetin, (c) L-dopa in the presence of MBTH, and (d) L-dopa in the presence of quercetin and MBTH. The wavelengths used and their respective molar absorptivity were (a) and (b), $\lambda = 475$ nm, $\epsilon_{475} = 3700$ $M^{-1}cm^{-1}$ (30); (c) and (d), $\lambda = 484$ nm, $\epsilon_{484} = 22300$ $M^{-1}cm^{-1}$ (30). The reaction medium contained (a) [L-dopa] = 2 mM, (b) [L-dopa] = 2 mM, [quercetin] = 0.2 mM, (c) [L-dopa] = 2 mM, [MBTH] = 3 mM, and (d) [L-dopa] = 2 mM, [quercetin] = 0.2 mM, [MBTH] = 3 mM. In all the cases, 50 mM sodium phosphate buffer pH 7.0 and $[E_0] = 1.74$ nM.

Scheme 2. Chemical Structure of the Evolution of Dopachrome to Indoles

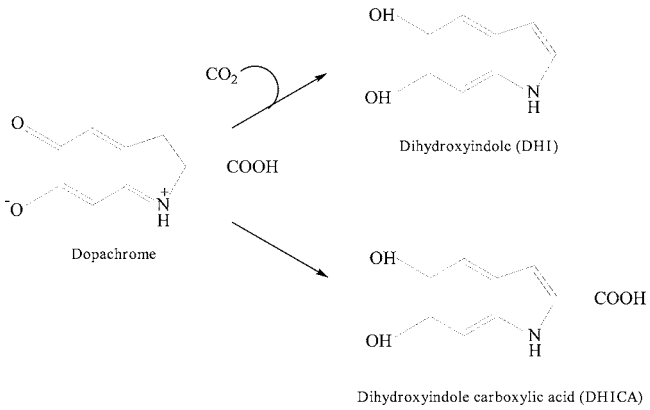

addition of MBTH, (**c**) and (**d**), respectively. Note that the trace without quercetin (**a**), shows a curvature at the time indicated in the figure (the concentrations of oxygen and L-dopa are not limiting): it is known that the product dopachrome is unstable and evolves to indoles (**Scheme 2**) (*29*). In the presence of quercetin (**b**), the kinetic is similar, but the observed absorbance is lower. In the presence of MBTH without quercetin (**c**) and with quercetin (**d**), the traces are more linear (*30*); however, in the presence of quercetin, the recorded absorbance is lower. Thus, although curves were obtained during the oxidation of L-dopa in the presence of quercetin, it is clear that this was not due to slow inhibition but rather to the instability of the dopachrome product (*29*).

To further this study, and taking **Figure 1** into account, we measured the initial rate of the oxidation of L-dopa in the absence and presence of quercetin. These results are shown in **Figure 3**, and the dependence obtained is of a rapid reversible competitive inhibitor type (similar to Figure 4 of ref 17).

Oxidation of Quercetin by Mushroom Tyrosinase. Figure 4 shows the oxidation of quercetin by mushroom tyrosinase.

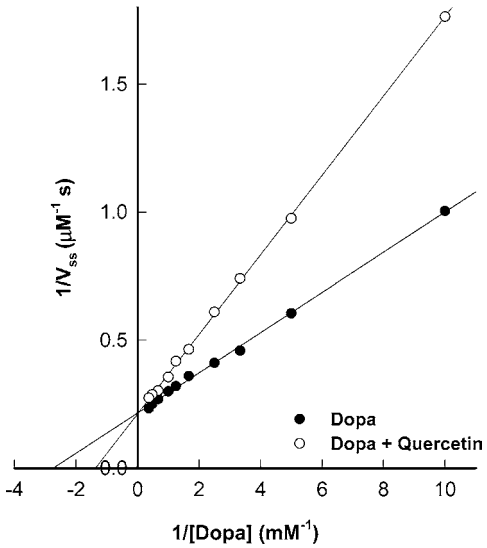

Figure 3. Lineweaver–Burk plots for the oxidation of L-dopa at 25 °C, pH 7.0 by mushroom tyrosinase in the absence (●) and presence (○) of quercetin (45 μM). The enzyme concentration was 43.6 nM in both cases. The initial rate measures were carried out spectrophotometrically recording dopachrome product at $\lambda = 515$ nm, to prevent the quercetin absorption (e = 2880 $M^{-1}cm^{-1}$).

The isosbestic points obtained indicate that the product (*o*-quinone) is stable in the absence of nucleophiles (**Scheme 3**). The **Figure 4** inset shows the kinetic traces ($\lambda = 375$ nm) for different substrate concentrations. These experiments indicate that quercetin is a substrate of mushroom tyrosinase. Thus, the interpretation of **Figures 2** and **3** becomes easier, in the sense that quercetin competes with L-dopa for tyrosinase.

Thus, in **Figure 2a**, the curvature is explained by the evolution of the dopachrome to indoles by the mechanism

$$\mathrm{S} \xrightarrow[\mathrm{O_2}]{V_0,\ \text{Tyrosinase}} \mathrm{Cr} \xrightarrow{k} \mathrm{I} \qquad (1)$$

where S represents L-dopa; Cr, dopachrome; and I represents DHI + DHICA (**Scheme 2**). The system rapidly reaches the steady-state with a rate V_0; thus, dopachrome is formed at a constant rate and is destroyed with an apparent constant k. The variation of Cr with time is the following:

$$\frac{\mathrm{d}[Cr]}{\mathrm{d}t} = V_0 - k[Cr] \qquad (2)$$

Integrating eq 2, and given [Cr] = 0 at t = 0, we obtain

$$[\mathrm{Cr}] = \frac{V_0}{k}(1 - e^{-kt}) \qquad (3)$$

For $t \rightarrow \infty$, [Cr] in the steady-state can be defined as

$$[\mathrm{Cr}]_{ss} = \frac{V_0}{k} \qquad (4)$$

From eqs 3 and 4 it is easily deduced that

$$\ln([\mathrm{Cr}]_{ss} - [\mathrm{Cr}]) = \ln[\mathrm{Cr}]_{ss} - kt \qquad (5)$$

Thus, the graphic representation of eq 5 predicts a linear slope k. These results are similar to those shown in Figure 5 of ref 17. Note that in that figure, a linear trace is proposed for the

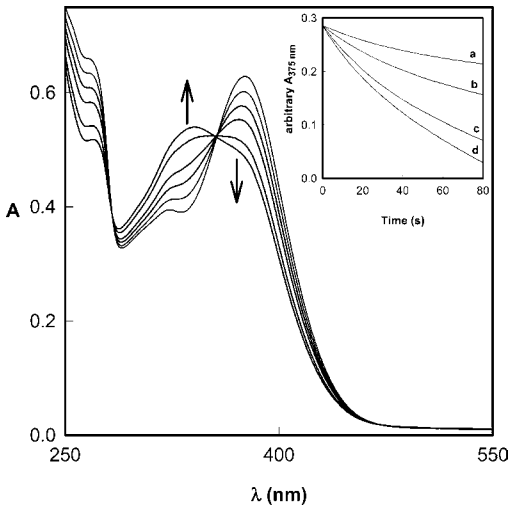

Figure 4. Consecutive spectra obtained for the oxidation of quercetin by mushroom tyrosinase. The assay medium contained 37 μM quercetin and 50 mM sodium phosphate buffer pH 7.0 at 25 °C. The reaction was started by addition of the enzyme (5.45 nM). Scans were recorded every 1 min during 10 min. Inset: Spectrophotometric recordings of the quinone formation by the action of tyrosinase on quercetin. The assay medium contained 50 mM sodium phosphate buffer pH 7.0, $[E_0] = 43.6$ nM, and the concentration of quercetin was (a) 15, (b) 30, (c) 60 and (d) 90 μM.

oxidation of L-dopa in the absence of quercetin. **Figure 2** shows the recorded trace in the presence of quercetin (**b**), which is similar to trace (**a**) but with a decreased absorbance, which can be explained if quercetin acts as competitive substrate of L-dopa, in accordance into the following mechanism:

$$\begin{array}{l} \mathrm{S} \overset{K_S}{\rightleftharpoons} \mathrm{ES} \xrightarrow{k_p} \mathrm{E} + \mathrm{Cr} \\ + \\ \mathrm{E} \\ + \\ \mathrm{S'} \overset{K_{S'}}{\rightleftharpoons} \mathrm{ES'} \xrightarrow{k_q} \mathrm{E} + \mathrm{Q} \end{array} \qquad (6)$$

where S represents L-dopa; Cr dopachrome, S′, quercetin; and Q, the *o*-quinone of quercetin. In this mechanism, the oxygen concentration has been omitted for simplicity, and two competitive substrates have been considered as originating Cr and Q products. By application of the steady-state approximation, the dopachrome formation rate is

$$V_{Cr} = \frac{k_p[S]_0[E]_0}{K_S\left(1 + \frac{[S']_0}{K_{S'}}\right) + [S]_0} \qquad (7)$$

By choosing a suitable wavelength where only Cr absorbs (515 nm), we obtain the data shown in **Figure 3**, in the presence and absence of quercetin. Analysis of this gives the kinetic parameters $V^S_{max} = (282 \pm 5.4)$ μM/min and $K_S = (0.36 \pm 0.01)$ mM in the absence of quercetin and $V^S_{max} = (282 \pm 5.9)$ μM/min and $K_S^{app} = (0.73 \pm 0.02)$ mM in the presence of quercetin, which confirms that quercetin acts as rapid reversible competitive substrate with L-dopa, and therefore, it is not a time-dependent inhibitor that acts with one or two steps, as has been described (*17*).

Once the action of mushroom tyrosinase on quercetin had been demonstrated (**Figure 4**), and with the aim of characterizing this substrate, a new spectrophotometric method was developed to measure the enzymatic activity, because at 375 nm, the substrate absorbance is too high and the concentration cannot be increased sufficiently to carry out the desired assay. Therefore, on the basis of previous studies on the measurement of the tyrosinase activity on different *o*-diphenols (*28*, *30*−*33*), we attempted to measure the formation of *o*-quinone adducts in the presence of different nucleophiles.

Oxidation of Quercetin by Tyrosinase in the Presence of Different Nucleophiles. (*a*) *Enzymatic Oxidation of Quercetin in the Presence of Cysteine.* **Figure 5** shows the iterative spectra of the oxidation of quercetin in the presence of cysteine, where the appearance of isosbestic points indicates a definite stoichiometry which corresponds to the change of substrate to adduct (**Figure 5**, **Scheme 3**) (*34*). However, the adduct spectrum is superimposed on the substrate spectrum and cannot be used quantitatively, although this did not occur with other substrates (*28*, *33*).

(*b*) *Enzymatic Oxidation of Quercetin in the Presence of MBTH.* To trap the *o*-quinones generated by tyrosinase during its action on different *o*-diphenols, several nucleophiles have

Scheme 3. Chemical Structure of the Oxidation of Quercetin by Tyrosinase in the Presence of MBTH and Thiol Compounds

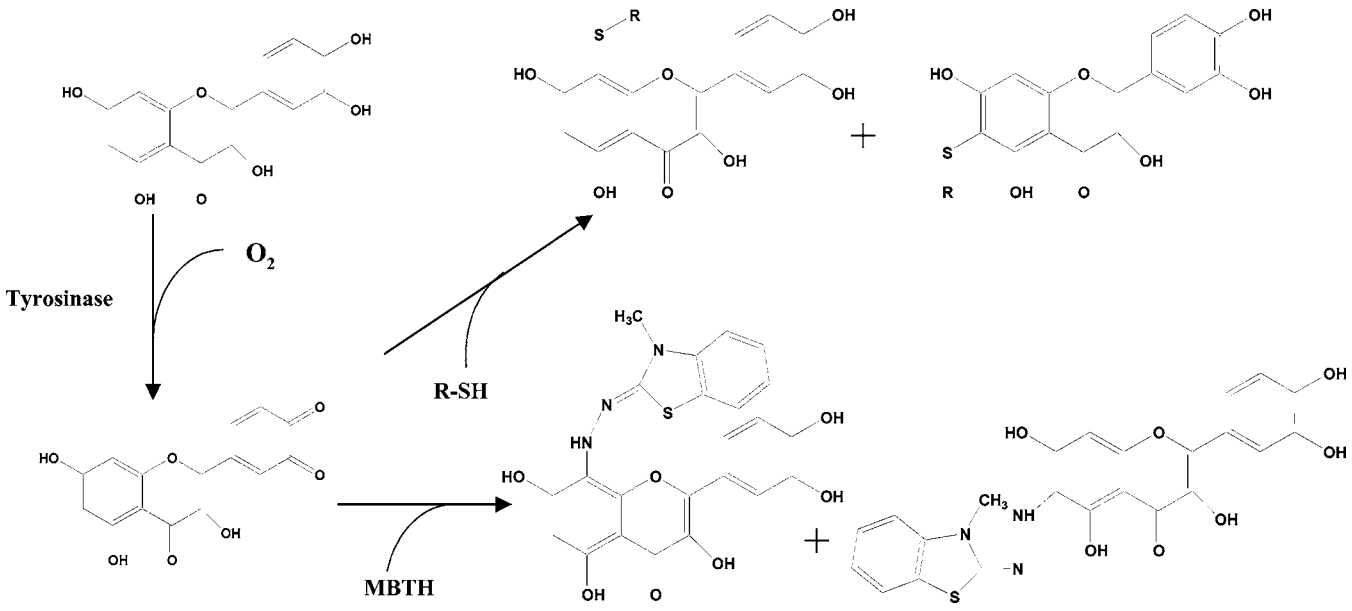

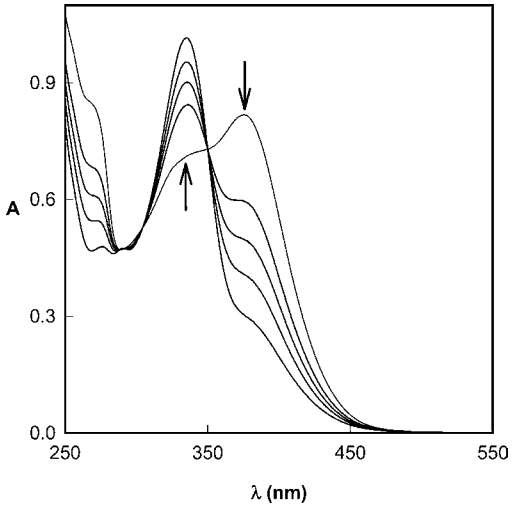

Figure 5. Consecutive spectra obtained in the oxidation of quercetin by mushroom tyrosinase in the presence of cysteine. The assay medium contained 60 μM quercetin, 1 mM cysteine, and 50 mM sodium phosphate buffer pH 7.0 at 25 °C. The reaction was started by addition of the enzyme (43.6 nM). Scans were recorded every 1 min during 10 min.

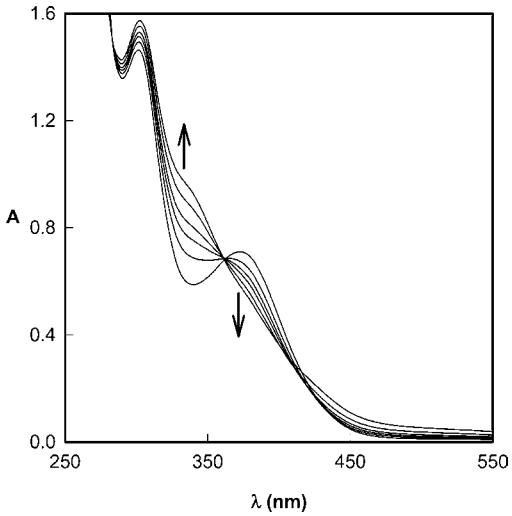

Figure 6. Consecutive spectra obtained in the oxidation of quercetin by mushroom tyrosinase in the presence of MBTH. The assay medium contained 45 μM quercetin, 0.2 mM MBTH, and 50 mM sodium phosphate buffer pH 7.0 at 25 °C. The reaction was started by addition of the enzyme (43.6 nM). Scans were recorded every 1 min during 10 min.

been used (*28*, *30*−*33*). Besthorn's hydrazone (MBTH) is a potent nucleophile, which has been used by our group to characterize several substrates of tyrosinase that give rise to very unstable *o*-quinones (*30*, *35*, *36*). Moreover, the chromophoric adducts formed have high molar absorptivity coefficients (*36*). However, in the case of quercetin, although the adduct is generated with a definite stoichiometry (**Figure 6**, **Scheme 3**) (*34*), a maximum does not appear in the visible part of the spectrum, meaning that it is not possible to obtain a high molar absorptivity coefficient in this zone. However, the extent of the adduct spectrum in the visible region permits measurements to be made without interference from the substrate.

Determination of the Molar Absorptivity Coefficient of the MBTH−Quercetin Adduct. Figure 7 shows the spectrophotometric recordings obtained using different concentrations of O_2 (*25*) and a high enzyme concentration. **Figure 7** Inset shows the linear ratio between A_{510} versus $[O_2]_0$. The slope of this straight line permitted the determination of the a molar

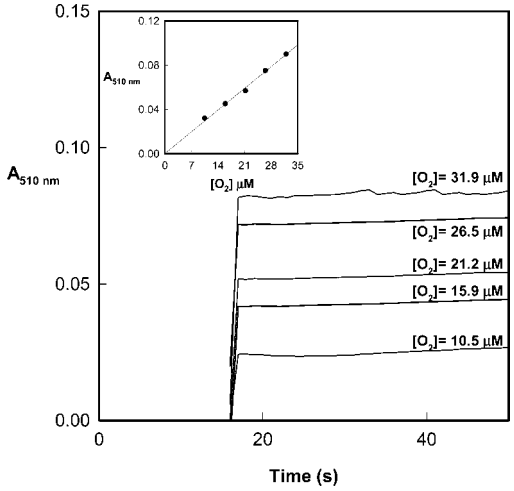

Figure 7. Determination of the molar absorptivity coefficient of the MBTH–quercetin adduct. Progress curves used to calculate the molar absorptivitie of the adduct (MBTH–quercetin) considering that 1 O_2 = 2 adduct. Assay conditions: 10.5, 15.9, 21.2, 26.5, and 31.9 μM of $[O_2]$, which correspond to 10, 15, 20, 25, and 30 μL of 2.18 μM mushroom tyrosinase, 0.3 mM quercetin in 50 mM sodium phosphate buffer, pH 7.0 at 25 °C. Inset: Absorbance obtained for each oxygen concentration vs the oxygen concentration.

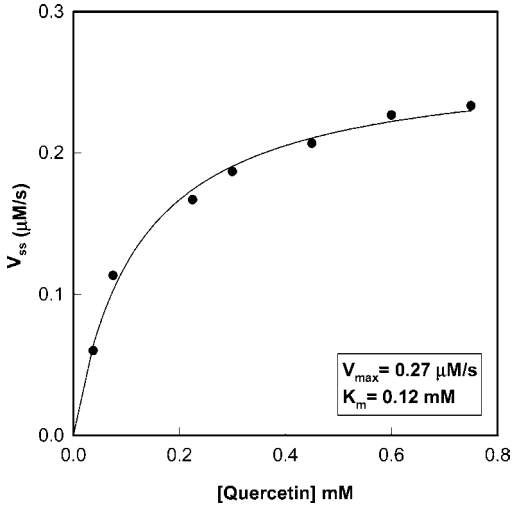

Figure 8. Dependence of quercetin oxidation on its concentration. The reaction medium contained quercetin at the indicated concentration, 2 mM MBTH and $[E_0]$ = 43.6 nM in 50 mM sodium phosphate buffer, pH 7.0. The quercetin oxidation was monitored by measuring the absorbance increasing at 510 nm.

coefficient absorptivity of 1509 $M^{-1}cm^{-1}$. The substrate does not absorb at 510 nm, which makes it possible to kinetically characterize the enzyme.

Kinetic Characterization of Mushroom Tyrosinase in its Action on Quercetin. The dependence of the quercetin oxidation rate on the quercetin concentration is shown in **Figure 8**, where the enzyme exhibits Michaelis−Menten type kinetics. Note the advantage of making measurements at 510 nm, a wavelength were it is possible to obtain initial rate values without interference from the substrate. The kinetic parameters obtained were V_{max} = (16.2 ± 0.6) μM/min and $K_{S'}$ = (0.12 ± 0.01) mM. From these values, the catalytic constant k_{cat} = (6.2 ± 0.6) s^{-1} was obtained in addition to a catalytic efficiency of 13.5 × 10^{-2} min^{-1}, similar to the catalytic efficiency obtained for broad bean tyrosinase (*37*).

The value obtained for the catalytic constant is very low and does not agree with the nucleophilic power of the *ortho*-hydroxylic groups of the substrate. On the other hand, the electron donating capacity (nucleophilic power) of the oxygen atom from different phenolic compounds has been correlated with the experimental ^{13}C NMR δ values for the carbon atom which supports the hydroxyl group (*38*). Thus, low δ values indicate high electronic density on this carbon atom and therefore a strongly nucleophilic oxygen atom. Thus, from the ^{13}C NMR spectrum we obtained the chemical displacement values at the C3′ ($\delta_{3'} = 147.87$), C4′ ($\delta_{4'} = 145.23$), and C3 ($\delta_3 = 122.18$) positions. The $\delta_{3'}$ and $\delta_{4'}$ values are comparable with the L-dopa values ($\delta_3 = 146.92$ and $\delta_4 = 146.06$) (*36*, *39*); therefore, the nucleophilicity of the hydroxyl groups is similar, and a k_{cat} value similar to L-dopa ($k_{cat} = 107.4 \pm 3.1$, ref 36) might be expected. However, the value obtained was 6.2 s^{-1}, which may be due to the large size of the molecule. This fact should have greater repercussions for $K_{S'}$ than k_{cat}, but in fact, the value obtained for $K_{S'}$ (0.12 ± 0.01) mM was lower than the value obtained for L-dopa (0.36 ± 0.01) mM (Figure 3). Nevertheless, note that the δ_3 value was very low ($\delta_3 = 122.18$), which means that the C3 oxygen acts as a potent nucleophile, and the ring containing C4 has an aromatic sextet if the two C=O electrons reside near the electronegative oxygen atom away from the ring (*40*). For this reason, both the oxygen of the hydroxyl group at the C3 position and the oxygen of the carbonyl group at the C4 position can bind the active site copper atoms to inhibit the enzyme. Thus, the compound could act as a substrate of the enzyme (*o*-diphenol) and an inhibitor at the same time, if it binds to the enzyme through the diphenolic site or through the pyrone ring, respectively. This situation can be represented as follows:

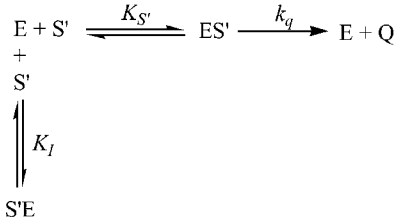

(8)

where K_I represents the dissociation constant of the substrate-enzyme complex bound through the pyrone ring (S′E) and $K_{S'}$ represents the dissociation constant of the enzyme−substrate complex bound through the diphenolic site (ES′). Applying the steady-state approximation, we obtain

$$V_0 = \frac{\dfrac{V_{max}}{1 + \dfrac{K_{S'}}{K_I}}[S']_0}{\dfrac{K_S'}{1 + \dfrac{K_{S'}}{K_I}} + [S']_0} = \frac{V_{max}^{app}[S']_0}{K_m^{app} + [S']_0} \qquad (9)$$

Equation 9 indicates that the experimental values of V_{max} and $K_{S'}$ are apparent (V_{max}^{app} and K_m^{app}), and are lower than the real values V_{max} and $K_{S'}$, which may explain the small values of k_{cat}^{app} and K_m^{app} obtained, although $V_{max}^{app}/K_m^{app} = V_{max}/K_{S'}$. Note that L-dopa oxidation in the presence of quercetin would now obey the steady-state rate expression described in eq 1A of the Appendix.

By studying the inhibition of tyrosinase by different flavonols (kaempferol, galangin, quercetin) (*16*, *17*), an inhibition mechanism involving copper chelation has been proposed for these substrates. All these compounds have a free 3-hydroxyl group in the *ortho*-position to a carbonyl group, a structure similar to that known for the inhibitors depicted in **Scheme 1**. However, the presence of a catechol moiety means that quecetin can also act as a substrate of mushroom tyrosinase. Moreover, this is confirmed by the fact that quercetin suppresses the lag period in the action of mushroom tyrosinase on L-tyrosine (*16*). However, it cannot be rejected that quercetin also binds to the enzyme through the catechol site or the pyrone moiety. In which case, we would be dealing with a compound that acts simultaneously as a substrate and an inhibitor.

In summary, a kinetic study of the action of mushroom tyrosinase on the flavonol quercetin reveals that this compound is a substrate of the enzyme, and possibly also a reversible and rapid competitive inhibitor.

APPENDIX

The action of mushroom tyrosinase on L-dopa (S) and quercetin (S′), assuming that quercetin binds to the enzyme at the diphenolic ring or at the pyrone ring:

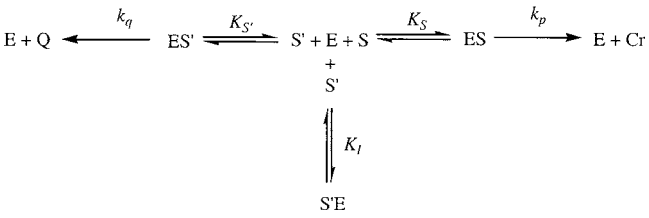

The dopachrome formation rate can be expressed as

$$V_{Cr} = \frac{k_p[E]_0[S]_0}{K_S\left[1 + \dfrac{K_I + K_{S'}}{K_I K_{S'}}[S']_0\right] + [S]_0} \qquad (1A)$$

LITERATURE CITED

(1) Mason, H. S. Comparative biochemistry of the phenolase complex. *Adv. Enzymol.* **1955**, *16*, 105−184.
(2) May, S. W. Applications of oxidoreductases. *Curr. Opin. Biotechnol.* **1999**, *10*, 370−375.
(3) Pawelek, J.; Chakraborty, A. K. The enzymology of melanogenesis. In *The Pigmentary System.*; Nordlund, J. J., Boissy, R., Hearing, V., King, R., Ortonne, J. P., Eds.; University Press.: Oxford, 1998.
(4) Prota, G. Progress in the chemistry of melanins and related metabolites. *Med. Res. Rev.* **1988**, *8*, 525−556.
(5) Prota, G.; d'Ischia, M.; Napolitano, A. The Chemistry of Melanins and Related Metabolites. In *The Pigmentary system*; Nordlund, J. J.; Boissy, R.; Hearing, V.; King, R.; Ortonne, J. P., Eds.; University Press.: Oxford, 1998.
(6) Solomon, E. I.; Sundaram, U. M.; Machonkin, T. E. Multicopper oxidases and oxygenases. *Chem. Rev.* **1996**, *96*, 2563−2605.
(7) Van Gelder, C. W. G.; Flurkey, W. A. Sequence and structural features of plant and fungal tyrosinases. *Phytochemistry* **1997**, *45*, 1309−1323.
(8) Vámos-Vigyázó, L. Prevention of enzymatic browning in fruits and vegetables: a review of principles and practice. In *Enzymatic Browning and its Prevention*; Lee, C. Y., Whitaker, J. R., Eds.; American Chemical Society: Washington, D. C., 1995.
(9) Walker, J. R. L. Enzymatic browning in fruits: its biochemistry and control. In *Enzymatic Browning and its Prevention*; Lee, C. Y., Whitaker, J. R., Eds.; American Chemical Society: Washington, D. C., 1995.

(10) Whitaker, J. R.; Lee, C. Y. Recent advances in chemistry of enzymatic browning: An overiew. In *Enzymatic Browning and its Prevention*; Lee, C. Y., Whitaker, J. R., Eds.; American Chemical Society: Washington, D. C., 1995.
(11) Zawistowski, J.; Biliaderis, C. G.; Michael-Eskin, N. A. Polyphenol Oxidase. In *Oxidative Enzymes in Foods.*; D. S. Robinson, N. A. M. Eskin, Eds.; Elsevier Science: London, 1991.
(12) Hollman, P. C.; Gaag, M.; Mengelers, M. J. B.; Trijp, J. M. P.; Vriers, J. H. M.; Katan, M. B. Absorption and disposition kinetics of the dietary antioxidant quercetin in man. *Free Radicals Biol. Med.* **1996**, *21*, 703−707.
(13) Lee, Y.; Howard, L.; Villalón, B. Flavonoids and antioxidant activity of fresh pepper (Capsicum annuum) cultivars. *J. Food Sci.* **1995**, *60*, 473−476.
(14) Gross, M.; Pfeiffer, M.; Martini, M.; Campbell, D.; Slavin, J.; Potter, J. The quantitation of metabolites of quercetin flavonols in human urine. *Cancer Epidemiol., Biomarkers Prev.* **1996**, *5*, 711−720.
(15) Okuda, T. Natural polyphenols as antioxidants and their potential use in cancer prevention. In *Polyphenolic Phenomena*; INRA: París, 1993.
(16) Kubo, I.; Kinst-Hori, I. Flavonols from saffron flower: tyrosinase inhibitory activity and inhibition mechanism. *J. Agric. Food Chem.* **1999**, *47*, 4121−4125.
(17) Chen, Q. X.; Kubo, I. Kinetics of mushroom tyrosinase inhibition by quercetin. *J. Agric. Food Chem.* **2002**, *50*, 4108−4112.
(18) Cabanes, J.; García-Carmona, F.; García-Cánovas, F.; Iborra, J. L.; Lozano, J. A. Kinetic study of the slow inhibition of epidermis tyrosinase by *m*-coumaric acid. *Biochim. Biophys. Acta* **1984**, *790*, 101−107.
(19) Cabanes, J.; García-Cánovas, F.; Tudela, J.; Lozano, J. A.; García-Carmona, F. L-Mimosine, a slow-binding inhibitor of mushroom tyrosinase. *Phytochemistry* **1987**, *26*, 917−919.
(20) Cabanes, J.; Chazarra, S.; García-Carmona, F. Kojic acid, a cosmetic skin whitening agent, is a slow-binding inhibitor of catecholase activity of tyrosinase. *J. Pharm. Pharmacol.* **1994**, *46*, 982−985.
(21) Espín, J. C.; Wichers, H. J. Slow-binding inhibition of mushroom (Agaricus bisporus) tyrosinase isoforms by tropolone. *J. Agric. Food Chem.* **1999**, *47*, 2638−2644.
(22) Duckworth, H. W.; Coleman, J. E. Physicochemical and kinetic properties of mushroom tyrosinase. *J. Biol. Chem.* **1970**, *245*, 1613−1625.
(23) Rodríguez-López, J. N.; Fenoll, L. G.; García-Ruiz, P. A.; Varón, R.; Tudela, J.; Thorneley, R. N.; García-Cánovas, F. Stopped-flow and steady-state study of the diphenolase activity of mushroom tyrosinase. *Biochemistry* **2000**, *39*, 10497−10506.
(24) Bradford, M. M. A rapid and sensitive method for the quatification of microgram quatities of proteins utilizing the principle of protein-dye binding. *Anal. Biochem.* **1976**, *72*, 248−256.
(25) Rodríguez-López, J. N.; Ros, J. R.; Varón, R.; García-Cánovas, F. Calibration of a clark-type oxygen electrode by tyrosinase-catalyzed oxidation of 4-*tert*-butylcathechol. *Anal. Biochem.* **1992**, *202*, 356−360.
(26) Fenoll, L. G.; Rodríguez-López, J.N.; Garcia-Molina, F.; García-Cánovas, F.; Tudela, J. Michaelis constants of mushroom tyrosinase with respect to oxygen in the presence of monophenols and diphenols. *Int. J. Biochem. Cell Biol.* **2002**, *34*, 332−336.
(27) Peñalver, M. J.; Rodríguez-López, J. N.; García-Molina, F.; García-Cánovas, F.; Tudela, J. Method for the determination of molar absorptivities of thiol adducts formed from diphenolic substrates of polyphenol oxidase. *Anal. Biochem.* **2002**, *309*, 180−185.
(28) Frieden, C. Analysis of kinetic data: practical applications of computer simulation and fitting programs. *Methods Enzymol.* **1994**, *240*, 311−322.
(29) Prota, G. Tyrosinase. In *Melanins and Melanogenesis*; Jovanovich, H. B., Ed.; Academic Press: San Diego, 1992.
(30) Rodríguez-López, J. N.; Escribano, J.; García-Cánovas, F. A continuous spectrophotometric method for the determination of monophenolase activity of tyrosinase using 3-methyl-2-benzothiazolinone hydrazone. *Anal. Biochem.* **1994**, *216*, 205−212.
(31) Cabanes, J.; García-Cánovas, F.; García-Carmona, F. Chemical and enzymatic oxidation of 4-methylcatechol in the presence and absence of L-serine. Spectrophotometric determination of intermediates. *Biochim. Biophys. Acta* **1987**, *914*, 190−197.
(32) Valero, E.; Escribano, J.; García-Carmona, F. Reactions of 4-methyl-o-benzoquinone, generated chemically or enzymatically, in the presence of L-proline. *Phytochemistry* **1988**, *27*, 2055−2061.
(33) Rodríguez-López, J. N.; Fenoll, L. G.; Peñalver, M. J.; García-Ruiz, P. A.; Varón, R.; Martínez-Ortíz, F.; García-Cánovas, F.; Tudela, J. Tyrosinase action on monophenols: evidence for direct enzymatic release of o-diphenol. *Biochim. Biophys. Acta* **2001**, *1548*, 238−256.
(34) Awad, H. M.; Boersma, M. G.; Boeren, S.; van der Woude, H.; van Zanden, J.; van Bladeren, P. J.; Vervoort, J.; Rietjens, I. M. C. M. Identification of o-quinone/quinone methide metabolites of quercetin in a cellular in vitro system. *FEBS Lett.* **2002**, *520*, 30−34.
(35) Espín, J. C.; Morales, M.; García-Ruiz, P. A.; Tudela, J.; García-Cánovas, F. Improvement of a continuous spectrophotometric method for determining the monophenolase and diphenolase activities of mushroom polyphenol oxidase. *J. Agric. Food Chem.* **1997**, *45*, 1084−1090.
(36) Espín, J. C.; Varon, R.; Fenoll, L. G.; Gilabert, M. A.; García-Ruiz, P. A.; Tudela, J.; Garcia-Canovas, F. Kinetic characterization of the substrate specificity and mechanism of mushroom tyrosinase. *Eur. J. Biochem.* **2000**, *267*, 1270−1279.
(37) Jiménez, M.; García-Carmona, F. Oxidation of the flavonol quercetin by polyphenol oxidase. *J. Agric. Food Chem.* **1999**, *47*, 56−60.
(38) Tomiyama, S.; Sakai, S.; Nihiyama, T.; Yasmada, F. Factors influencing the antioxidant activities of phenols by an ab initio study. *Bull. Chem. Soc. Jpn.* **1993**, *66*, 205−211.
(39) Fenoll, L. G.; Rodríguez-López, J. N.; García-Sevilla, F.; García-Ruiz, P. A.; Varón, R.; García-Cánovas, F.; Tudela, J. Analysis and interpretation of the action mechanism of mushroom tyrosinase on monophenols and diphenols generating highly unstable o-quinones. *Biochim. Biophys. Acta* **2001**, *1548*, 1−22.
(40) Smith, M. B.; March, J. In *March's Avanced Organic Chemistry Reactions, Mechanisms, and Structure*, 5th ed.; A. Wiley-Interscience: New York, 2001, p 53.

Received for review June 20, 2003. Revised manuscript received September 23, 2003. Accepted October 8, 2003. This work was supported in part by grants from the MCYT (Spain) Project AGL2002-01255 ALI and from the Fundación Séneca/Consejería de Agricultura, Agua y Medio Ambiente (Murcia) Project AGR/10/FS/02. L.G.F. has a fellowship from the University of Murcia.

JF034656Y